

# Effect of Vacancy Defect on Natural Vibration of Single Walled Carbon Nanotube as Ultrahigh Nanoresonators

Mojtaba Amjadipour\*. Ardeshir Karami Mohammadi\*\*

\*mechanical engineering department, Shahrood University of Technology,  
Shahrood, Iran (email: amjadipour.mojtaba@gmail.com)

\*\*mechanical engineering department, Shahrood University of Technology,  
Shahrood, Iran (email: akaramim@yahoo.com)

---

**Abstract:** This paper presents the effect of vacancies on natural vibration of single walled carbon nanotubes. Molecular dynamic model and finite element method are used to simulate SWCNTs. Related stiffness is calculated from molecular potential energy. Vacancies are scattered randomly on SWCNT structure for better simulation of actual condition. SWCNTs are good candidate for high frequency actuator because of their high natural frequencies. Accurate prediction of principle frequency of resonators affects their operation. Vacancy defects occurs during growth process, so determining natural frequency of defected SWCNTs as actuators is very important for improving their performance. Zigzag carbon nanotube with chirality indices (8,0) and (10,0) are considered. Accuracy of modeling is verified by comparing our results of predicting ideal SWCNT natural frequency, with results of previous studies. Effects of aspect ratio, diameter, distribution of vacancies, and boundary conditions on natural vibration of defected SWCNTs are investigated. Our results indicate that by decreasing aspect ratio and CNT diameter, natural vibration frequency shift increases. Distribution of vacancies affects natural frequency shift. As vacancies approach to the clamped end, natural frequency shift increases.

Keywords: Molecular Dynamics, Nano-Science, Vacancy Defect, Natural Vibration.

---

## 1. INTRODUCTION

Carbon nanotubes possess superior properties such as ultra high strength, high electrical and thermal conductivity, high natural frequency due to their ideally perfect structures (Treacy et al. (1996), Ebbesen et al. (1996), Li et al. (2003(a))). Resonators are key components in signal processing systems (Los Santos (1999)). Reduction in the size of a resonator enhances its resonant frequency and reduces its energy consumption (Los Santos (1999)). For sensors, higher resonant frequency means higher sensitivity (Jensen et al. (2008)). For wireless communications, higher frequency resonators enable the production of higher frequency filters, oscillators, and mixers (Los Santos (1999)). CNTs have favorable properties, such as extremely high in-plane elastic modulus, high natural frequency and thermal conductivity. These properties, combined with their nanometer-sized, perfect atomic structure, imply that CNTs have potential applications in nano-electromechanical systems, such as components for high frequency oscillators in sensing and signal processing applications (Poncharal et al. (1999), Jensen et al. (2008)).

Poncharal (1999) demonstrated the use of the resonance of a cantilevered CNT to estimate the mass of an attached carbonaceous as light as 30 fg inside a transmission electron microscope. Jensen et al. (2008) demonstrated a room-temperature, CNT-based nanomechanical resonator with atomic mass resolution, based on a nanotube radio receiver design. The potential of double-walled CNTs (DWCNTs) as

nanoresonators have been explored, using an atomistic modeling technique (Kang et al. (2009)).

Meanwhile, the defects in nanotubes, including substitutional impurities, vacancies, and topologic defects, etc. (Choi et al. (2000), Suenaga et al. (2007), Alexandre et al. (2008)) create heterogeneous structures, which can change the electronic, chemical, and mechanical properties of the carbon nanotubes, and in consequence, seriously influence their applications in nanoelectro-mechanical systems (NEMS) and nanocomposites (Wang et al. (2006(a, b)), Park et al. (2007), kang et al. (2009), HaiYun and Tao (2010)).

The Stone-Wales (SW) defects (namely twinned pentagon heptagon pairs (Stone (1986))) and vacancies are typical defects observed in carbon nanotubes. For example, it was suggested that 2%–5% carbon atoms are involved in SW defective sites (Monthieux (2002)). Zhou et al. (2007) investigated the transport properties of defected zigzag metallic single-walled nanotubes (SWNTs), and found that the circumferential interference dependent on the defect configuration is responsible for the transport blocking observed experimentally (Gómez-Navarro et al. (2005)). Tunvir et al. (2008) studied the mechanical properties of SWNTs having two neighboring vacancy defects or SW defects, and found that the defect configuration in the SWNT structure is one of the key factors in determining its mechanical properties, as well as the population of defects. Barinov et al. (2007) and Kim et al. (2007) studied the adsorption and transport of metallic atoms on multi-walled carbon nanotubes (MWNTs). The diffusion mechanism of

indium atoms along MWNTs was revealed by means of photoemission spectromicroscopy and density functional theory calculations: the indium transport is controlled by the concentration of defects in the C network and proceeds via hopping of indium adatoms between C vacancies (Barinov et al. (2007)). The calculations of Pt nanoparticles loaded on the defective carbon nanotubes showed that the adsorption of Pt atom on the vacancy of nanotube was significantly stronger by s-p hybridization with carbon atoms near the defect site (Kim et al. (2007)). It is well believed that the defect configurations may seriously influence the mechanical and electrical properties of carbon nanotubes (HaiYun and Tao (2010)).

## 2. MODELING

In this paper molecular dynamic model is used. The basic premise in this method is that CNT can be modeled as a continuum having continuous distributions of mass and stiffness (Gibson et al. (2007)). Odegard et al. (2002) used an equivalent continuum model for prediction of structural property of nanostructure materials. Bending rigidity of graphene sheet was determined based on this method (Gates et al. (2005)). Extensional, torsional and bending rigidity of SWNTs was determined using the potential energy for the interatomic forces of a molecular mechanics model (Bodily et al. (2003)).

Li & Chou (2003(a, b)) developed a similar method using continuum mechanic and molecular dynamic for predicting static and dynamic properties of CNTs. Thus we can simulate a SWCNT as a space frame consist of mass and stiffness.

The most part of atom's mass is related to nucleus so nucleus mass ( $m_c = 1.9943 \times 10^{-26} \text{ Kg}$ ) is considered as atom's mass and Electron masses are neglected.

Mass element is located on carbon atom position in CNT structure for simulation of atoms mass. Bonding of carbon atoms is modeled by elastic stiffness element (Li & Chou (2003(a, b))).

Fig. 1 shows the interatomic interactions modeled with this approach.

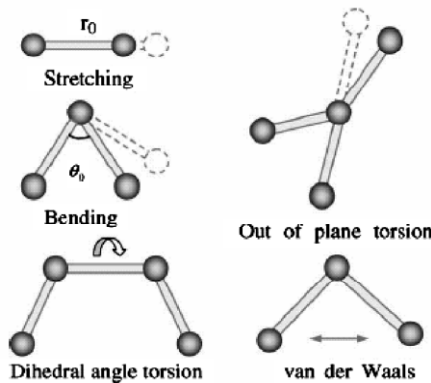


Fig. 1. interatomic interaction

Total steric potential energy was expressed as sum of energies due to valance or bonded interactions and nonbonded interactions (Rappe (1992)).

$$U = \sum U_r + \sum U_\theta + \sum(U_\varphi + U_\omega) + \sum U_{VDW} \quad (1)$$

where  $U_r$ ,  $U_\theta$ ,  $U_\varphi$ ,  $U_\omega$  and  $U_{VDW}$  are the energy terms due to bond stretching, bond angle bending, dihedral angle torsion, out-of-plane torsion and van der Waals interaction, respectively.

In this research we omitted the term related to van der Waals interaction. So (1) can be expressed as

$$U = \sum U_r + \sum U_\theta + \sum(U_\varphi + U_\omega) \quad (2)$$

Where:

$$U_r = \sum_{bonds} \frac{1}{2} k_r (r - r_{eq})^2 \quad (3)$$

Where  $k_r$  is the bond stretching force constant,  $r$  is the distance between atoms,  $r_{eq}$  is the equilibrium distance between atoms.

$$U_\theta = \sum_{angles} \frac{1}{2} k_\theta (\theta - \theta_{eq})^2 \quad (4)$$

Where  $k_\theta$  is the bond-angle bending force constant,  $\theta$  is the bond angle,  $\theta_{eq}$  is the equilibrium bond angle.

$$U_\varphi + U_\omega = \sum_{dihedral} \frac{1}{2} k_\tau (\varphi - \varphi_{eq})^2 \quad (5)$$

Where  $k_\tau$  is torsional resistance constant,  $\varphi$  is the torsion angle and  $\varphi_{eq}$  is the equilibrium torsion angle (Odegard et al. (2002)).

From structural mechanic view point, potential energy for elastic beam element can be expressed as:

$$U = \sum U_p + \sum U_M + \sum U_T \quad (6)$$

Where  $U_p$ ,  $U_M$  and  $U_T$  are strain energies for axial tension, bending and torsion respectively.

So we can simulate related molecular potential energy with mechanical element potential energy. From equivalence of energies in (2) and (6), force filed space frame model is created. Beam element characteristics can be expressed by molecular mechanic constants as in (7).

$$k_r = EA/L, k_\theta = EI/L, k_\tau = GJ/L \quad (7)$$

The force constant values are chosen based upon the experience with graphite sheets:  $\frac{k_r}{2} = 469 \text{ kcal mol}^{-1} \text{ \AA}^{-2}$ ,  $\frac{k_\theta}{2} = 63 \text{ Kcal mol}^{-1} \text{ rad}^{-2}$ . The force constant  $k_\tau$  is adopted as  $\frac{k_\tau}{2} = 20 \text{ Kcal mol}^{-1} \text{ rad}^{-2}$  based on results of Cornell et al. (1995). The capability and efficiency of this molecular structural mechanics method have been verified in the modeling of single walled carbon nanotubes under tension or torsion. The calculated results of Young's modulus and shear modulus are in good agreement with the theoretical predictions and experimental results available in the literature (Li & Chou (2003(b))).

For vacancy simulation, related elements were omitted in frame like model.

## 3. ANALYSIS METHOD

For the free vibration of undamped structure problem, the equation of motion is

$$[M]\{\ddot{y}\} + [K]\{y\} = 0 \quad (8)$$

Where  $[M]$  and  $[K]$  are, respectively, the global mass and stiffness matrices, and  $\{y\}$  and  $\{\ddot{y}\}$  are respectively the nodal displacement vector and acceleration vector.

The global stiffness matrix  $[K]$  of the frame structure can be assembled from the elemental stiffness matrix  $[K] = \sum_{e=1}^n [K]^e$  where  $n$  is the number of elements. For assembling nodes, finite element method was used. According to modeling,  $[K]^e$  can be expressed as

$$[K]^e = \begin{bmatrix} [k_{ii}] & [k_{ij}] \\ [k_{ji}] & [k_{jj}] \end{bmatrix} \quad (9)$$

Where submatrices  $[k_{ii}]$ ,  $[k_{ij}]$ ,  $[k_{ji}]$  and  $[k_{jj}]$  express related stiffness of element  $i$ - $j$ .

The global mass matrix  $[M]$  can be obtained from elemental mass matrix.

The coefficient in the mass matrix corresponding to flexural rotation and torsional rotation  $\frac{2}{3}m_c r_c^2$ , are assumed to be zero because of the extremely small radius of SWCNTs. Only the coefficient corresponding to translator displacements are kept. Thus the elemental mass matrix is expressed as

$$[M]^e = \text{diag} \left[ \frac{m_c}{3} \quad \frac{m_c}{3} \quad \frac{m_c}{3} \quad 0 \quad 0 \quad 0 \right] \quad (10)$$

The factor  $\frac{1}{3}$  is introduced because of the three bonds of carbon atom connecting with the three nearest neighboring atoms. The natural frequencies  $f$  and mode shapes are determined from the solution of the eigenproblem

$$([K]_s - \omega^2 [M]_s) \{y_p\} = 0 \quad (11)$$

Where  $[K]_s$  and  $[M]_s$  are the condensed stiffness and mass matrix, respectively,  $\{y_p\}$  is the displacement vector, and  $\omega = 2\pi f$  is the angular frequency (Li & Chou (2003(a))).

#### 4. RESULTS

For validation of the modeling technique, the results were compared with Li and Chou's (2003(a)) in Fig. 2. Perfect SWCNT with chirality index (8,0) and bridged boundary condition was considered.

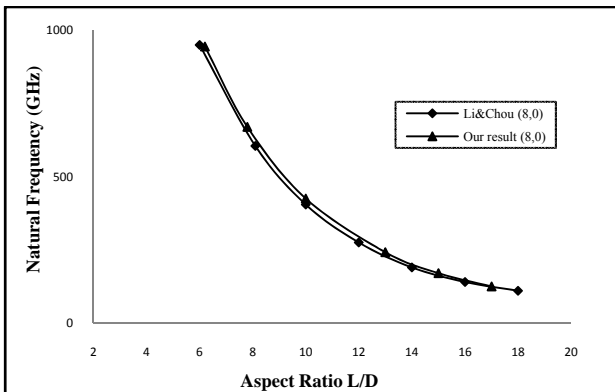


Fig. 2. Comparison the present results with Li and Chou's result for perfect SWCNT (8,0)

As Fig. 2 shows, our results are close to those of Li and Chou (2003(a)).

Fig. 3 shows five SWCNTs mode shapes.

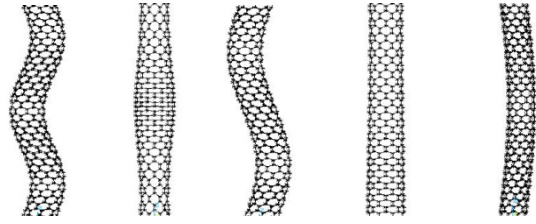


Fig. 3. Five SWCNTs mode shapes

For investigating vacancy defect effect on natural frequency of SWCNTs we create vacancies randomly on CNT's structure with different ratio. So  $\frac{n_1}{n} \times 100$  has been defined to express amount of vacancies. Where  $n_1$  explains number of nodes that have been vanished due to vacancy modeling and  $n$  is number of total nodes in CNT's structure. Creation of random vacancies has two limitations. First, two neighbor nodes cannot be eliminated together. Second, distribution of vacancies should be uniform. Fig. 4 shows natural vibration frequency shift of SWCNT with chirality index (8,0). Cantilevered boundary condition with different aspect ratio and different vacancy ratio has been considered.

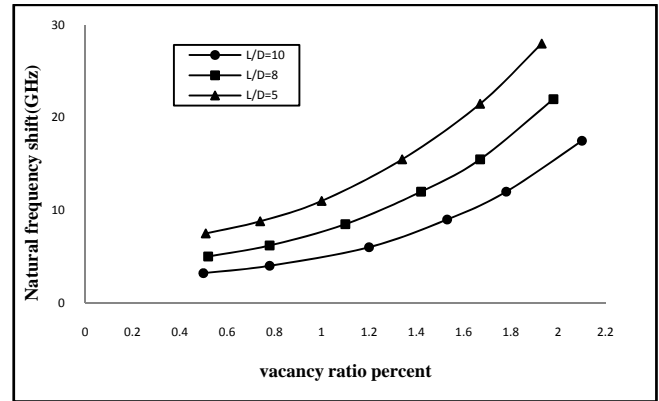


Fig. 4. Natural frequency shift of SWCNT (8,0) with cantilevered boundary condition.

As Fig. 4 shows, SWCNT with vacancy ratio equal to 2 percent and aspect ratio equal to 5 has natural frequency approximately 28 GHz less than perfect one. So vacancies affect principle frequency of nanotube extremely. It's clear from Fig. 4 that as vacancy ratio increases, frequency shift increases too. When vacancy ratio percent is equal or more than 0.85 the slope of diagram increases. this condition indicates that from this point on, the effect of vacancies on principle frequency increases. When nanotube length decreases natural frequency shift increases.

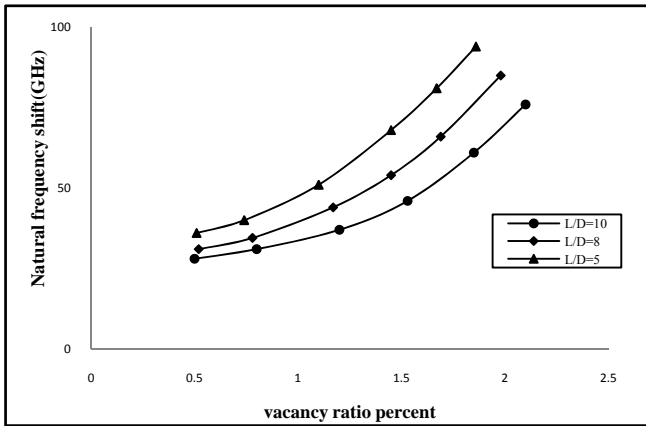


Fig. 5. Natural frequency shift of SWCNT (8,0) with bridged boundary condition.

Fig. 5 indicates that for SWCNT when vacancy ratio is 1.88 and aspect ratio is 5, natural frequency shift is equal to 96 GHz. It's clear from Fig. 5 that relation between diameter and length and frequency shift is the same as Fig. 4. By comparing Fig. 4 and Fig. 5 we can understand that boundary condition affects the vacancy defect effect on principle frequency of SWCNTs. Natural frequency shift in bridged boundary condition is more than cantilevered one.

Effect of vacancies on natural vibration of SWCNT with chiral index (10,0) has been studied and results are shown in the Fig. 6.

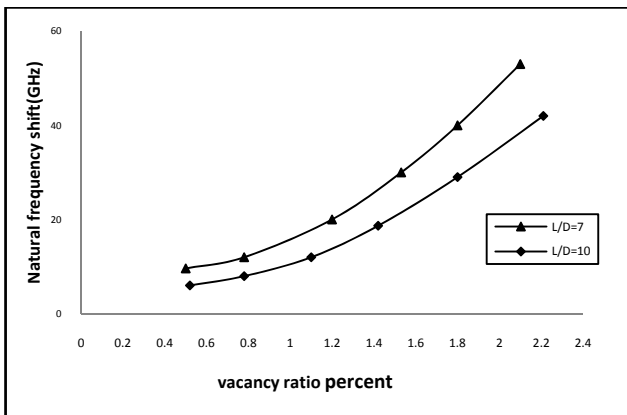


Fig. 6. Natural frequency shift for SWCNT (10,0) with bridged boundary condition

When vacancy ratio of SWCNT is equal to 2.1 percent and its aspect ratio is equal to 7, its natural frequency is approximately 54 GHz less than perfect one. By increasing length and diameter of nanotube natural frequency shift decreases. When vacancy ratio is equal or more than 0.9, amount of vacancy effect increases

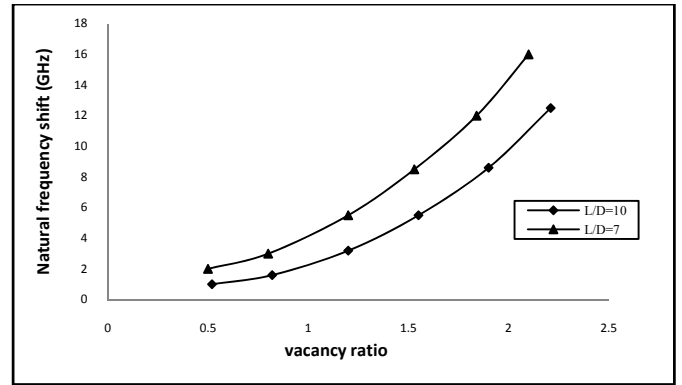


Fig. 7. Natural frequency shift for SWCNT (10,0) with cantilevered boundary condition

Fig. 7 indicates that for SWCNT when vacancy ratio is 2.1 and aspect ratio is 7, natural frequency shift is equal to 17 GHz. It's clear from Fig. 7 that natural frequency shift decreases when diameter and length increases. By comparing Fig. 6 and Fig. 7 we can understand that boundary condition affects the vacancy defect effect on principle frequency of SWCNTs. Natural frequency shift in bridged boundary condition is more than cantilevered one.

Position of defects affects the natural frequency too. When vacancies are nearer to the clamped end, amount of SWCN natural frequency shift increases.

## 5. CONCLUSION

Using the molecular mechanic method, we investigate vacancy defect effect on natural vibration of SWCNTs with chiral indices (8,0), (10,0). Results indicate that vacancies affect fundamental frequency of single walled carbon nanotubes. Boundary condition, aspect ratio and distribution of vacancies affect natural frequency shift. When vacancy ratio is approximately less than 0.7, slope of natural frequency shift is approximately zero. It means that if we can hold vacancy ratio during growth process less than 0.8, fundamental frequency shift will be minimized.

## REFERENCES

- Alexandre S S, Mazzoni M S C, Chacham H (2008). Edge states and magnetism in carbon nanotubes with line defects. *Phys Rev Lett*,100: 146801.
- Barinov A, Üstünel H, Fabris S, et al (2007). Defect-controlled transport properties of metallic atoms along carbon nanotube surfaces. *Phys Rev Lett*, 99: 046803.
- Bodily BH, Sun CT (2003). Structural and equivalent continuum properties of single-walled carbon nanotubes. *Int J Mater Product Technol*;18(4/5/6):381–97.
- Choi H J, Ihm J, Louie S G, et al (2000). Defects, quasibound states, and quantum conductance in metallic carbon nanotubes. *Phys Rev Lett*, 84: 2917–2920.
- W.D. Cornell, P.Cieplak et al (1995). *Journal of the American Chemical Society* 117. 5179.
- H. J. De Los Santos (1999). *Introduction to Microelectromechanical Microwave Systems*. Artech House Publishers, London.

- Ebbesen T W, Lezec H J, Hiura H, et al (1996). Electrical conductivity of individual carbon nanotubes. *Nature*, 382: 54–56.
- Gates TS, Odegard GM, Frankland SJV, Clancy TC (2005). Computational materials: multi-scale modeling and simulation of nanostructured materials. *Compos Sci Technol*;65(15 16):2416–34.
- Gómez-Navarro C, De Pablo P J, Gómez-Herrero J, et al (2005). Tuning the conductance of single-walled carbon nanotubes by ion irradiation in the Anderson localization regime. *Nat Mat*, 4: 534–539.
- Qian HaiYun, Zhou Tao (2010). Electronic properties of multi-defected zigzag carbon nanotubes. *Sci China Phys Mech Astron*. Vol. 53: 11-15.
- K. Jensen, K. Kim, A. Zettl (2008). *Nature Nanotechnology* 3. 533.
- Jeong Won Kang, Oh Kuen Kwon, Jun Ha Lee, Young Gyu Choi, Ho Jung Hwang (2009). Frequency change by inter-walled length difference of double-wall carbon nanotube resonator. *Solid State Communications* 149. 1574\_1577.
- Kim S J, Park Y J, Ra E J, et al (2007). Defect-induced loading of Pt nanoparticles on carbon nanotubes. *Appl Phys Lett*, 90: 023114.
- Li C, Chou T-W (2003(a)). Single-walled nanotubes as ultrahigh frequency nanomechanical resonators. *Phys Rev B*;68:073405. [5 modeling]
- Li C, Chou T-W (2003(b)). A structural mechanics approach for the analysis of carbon nanotubes. *Int J Solids Struct*;40:2487–99.
- Monthioux M (2002). Filling single-wall carbon nanotubes. *Carbon*, 40: 1809–1823.
- Odegard GM, Gates TS, Nicholson LM, Wise KE (2002). Equivalent continuum modeling of nano-structured materials. *Compos Sci Technol*;62:1869–80.
- Park J Y (2007). Electrically tunable defects in metallic single-walled carbon nanotubes. *Appl Phys Lett*, 90: 023112.
- P. Poncharal, Z.L. Wang, D. Ugarte, W.A. de Heer (1999). *Science* 283. 1513.
- A. K. Rappe (1992). *J. Am. Chem. Soc.* 114, 10024.
- Ronald F. Gibson , Emmanuel O. Ayorinde , Yuan-Feng Wen (2007). Vibration of carbon nanotubes and their composites: A review. *Composite Science*.
- Stone A J, Wales D J (1986). Theoretical studies of icosahedral C<sub>60</sub> and some related species. *Chem Phys Lett*, 128: 501–503.
- Suenaga K, Wakabayashi H, Koshino M, et al (2007). Imaging active topological defects in carbon nanotubes. *Nature*, 2: 358–360.
- Treacy M M J, Ebbesen T W, Gibson J M (1996). Exceptionally high Young's modulus observed for individual carbon nanotubes. *Nature*, 381: 678–680.
- Tunvir K, Kim A, Nahm S H (2008). The effect of two neighboring defects on the mechanical properties of carbon nanotubes. *Nanotechnology*, 19: 065703.
- Wang C C, Zhou G, Wu J, et al (2006(a)). Effects of vacancy-carboxyl pair functionalization on electronic properties of carbon nanotubes. *Appl Phys Lett*, 89: 173130.
- Wang C C, Zhou G, Liu H T, et al (2006(b)). Chemical functionalization of carbon nanotubes by carboxyl groups on Stone-Wales defects: A density functional theory study. *J Phys Chem B*, 110: 10266–10271.
- Zhou T, Wu J, Duan W H, et al (2007). Physical mechanism of transport blocking in metallic zigzag carbon nanotubes. *Phys Rev B*, 75:205410.